THE UNIVERSITY of TULSA

TUDRP

The University of Tulsa
Drilling Research Projects

Experimental Study and Modeling of Yield Power-Law Fluid Flow in Pipes and Annuli (Effects of Drillpipe Rotation)

Ramadan Ahmed, The University of Tulsa, Drilling Research Projects

This report is prepared for TUDRP Advisory Board Meeting, Nov. 13-14, 2006, Tulsa, Oklahoma

Summary

This is the fourth report, which presents experimental studies on the flow of YPL fluids in both concentric and eccentric annuli with pipe rotation. The report includes literature review and experimental investigations. At the last TUDRP Advisory Board Meeting (May 2006), the third report was presented. The report covered modeling study and experimental investigation on laminar flow of Yield Power-Law (YPL) fluids in concentric annuli with pipe rotation.

Field measurements carried out in recent years have indicated that the annular pressure loss can depend significantly on the rotational speed of the drillpipe. For this reporting period, major emphasis is given to the effect of drillpipe rotation in concentric and eccentric annuli. Extensive flow experiments with polymer-based fluids were carried out using the dynamic testing facility (Fig. 1). Three annular geometries have been considered for the investigation. Five different formulations of test fluid (Table 1) were prepared by varying concentrations of Xanthan Gum (XCD) and Polyanionic Cellulose (PAC) for each annular geometry. Flow rate and rotational speed were varied from 2 gpm [7.56 l/min] to 21.91 [82.82 l/min] and 0 rpm to 400 rpm, respectively. Fluid characterization was made using horizontal pipe sections and a rotational viscometer.

Experimental results indicate the presence of shear thinning and inertial effects when inner pipe rotates. In highly eccentric annuli, inertial effects dominate the phenomenon of shear thinning and result in increased pressure loss as the speed increases. Inertial effects can be generated due eccentricity and/or geometric irregularities of the annulus that substantially influence the velocity field as the pipe rotates. The experimental data obtained from the flow loops, field measurements and results from theoretical analysis will be used to develop a hydraulic model that accounts for drillpipe rotation.

Introduction

Many modern drilling fluids such as synthetic/polymer based muds are of Yield Power-Law type fluids.[1] Polymer based muds that have Yield Power-Law rheology are widely used in drilling operations with well-known benefits.[2] Currently, very limited hydraulic data is available for such fluids. The rheology and hydraulics of these fluids are very essential for the design of hydraulic programs, cuttings transport and drilling optimization.

The overall aim of this study is to develop reliable hydraulic models that accurately predict the frictional pressure losses in pipes and annuli under laminar, transitional and turbulent flow conditions. The research involves both mathematical modeling and experimental investigations. The effects of fluid properties (function of temperature and pressure), eccentricity, pipe roughness and pipe rotation on the relationship between frictional pressure losses and flow rate will be studied experimentally and theoretically.

Fig. 1 Dynamic Testing Facility (DTF)

Previous lab experimental results[3-9] and field measurements[10-18] indicated that the effect of pipe rotation on friction pressure loss is considerable and depended on fluid properties (rheology and density), flow regime, diameter ratio and eccentricity. In addition, annular pressure loss prediction requires the knowledge of flow pattern/regime, when the inner pipe rotates in the annulus. This is especially critical for drilling slimholes because small variations in annular gap or eccentricity or pipe rotational speed strongly affect the pressure loss. The change in friction pressure loss due pipe rotation is attributed to different flow phenomena such as:

i. Shear Thinning: Shear thinning in non-Newtonian flows tends to reduce the friction pressure loss due to the coupling of axial and rotational flow through shear rate dependent apparent viscosity function.

ii. Inertial/Acceleration Effects: Inertial effects can be generated due the eccentricity or geometric irregularities of the annulus. As the pipe rotates, the geometric irregularities tend to change the

eccentricity and skewness of the drillpipe at a specific depth. A continuous change in the annular geometry results in an increase in friction pressure loss. Moreover, in eccentric annulus, pipe rotation generates very complicated flow patterns (secondary flows), resulting in substantial variation of the velocity (both magnitude and direction) of a fluid element (inertial effect) along the streamline and an increase in the friction pressure loss.

iii. Secondary Flows: Due to centrifugal and shear-instabilities, secondary flows patterns such as Taylor vortices can be formed in annular flows and increase the friction pressure loss.

Objective

The primary objective of this research project is to conduct an experimental and theoretical study of the rheology and hydraulics of YPL (synthetic/polymeric) fluids under different temperature and pressure conditions (simulated downhole conditions). The overall objectives of the project are clearly stated in the research proposal. The specific objectives for this part of the investigation will be:

i) to investigate experimentally and theoretically the effect of pipe rotation on annular pressure loss;
ii) to study stability characteristics of helical flows in annuli;
iii) to develop hydraulic models that account for the effect pipe rotation;
iv) to present experimental database for flow of polymeric (YPL) fluids in annuli with pipe rotation;
v) to study and identify flow patterns/structures in helical flow of YPL fluids.

Scope of Work and Methodology

The overall scope of the research was presented in detail in the proposal. It includes experimental investigations and theoretical/numerical simulation studies on pipe and annular flows of YPL fluids under laminar, transition and turbulent flow conditions. The scope of the current investigation includes:

i) Literature review on laminar flow of YPL fluid in concentric annuli with pipe rotation;
ii) Experimental investigation of polymeric (YPL) fluid flow in annuli with pipe rotation;
iii) Mathematical modeling of YPL fluid flow in concentric annuli with pipe rotation;
iv) Comparison of experimental measurements with predictions of mathematical models.

Literature review

A number of investigators studied the pressure losses in the annulus and the effect of pipe rotation over the years. Recently, due to the introduction of new drilling technologies such as slim-hole and casing drilling applications, the concern about the effect of pipe rotation on annular frictional pressure loss has motivated new

researches on this subject. In the past, theoretical studies were conducted to present a solution for helical flow of non-Newtonian fluids in a concentric annulus; and recently, some experimental and field studies have been performed.

Several studies[4,6-8,13,19] reported the reduction of pressure loss due to drillstring rotation. However, a number of investigators[3,5-15,20] observed significant increase in pressure loss as drillstring rotates at higher speeds.[20] Different explanations have been presented to describe the effect of pipe rotation including: shearing thinning, flow regime transition from laminar to turbulent, formation of Taylor vortices, drill pipe eccentricity and wobbling effects, suspension of cuttings and tool joint effect.[17] In general, field measurements showed increased pressure loss as the rotation speed increases.

A number of numerical studies[21-25] were performed to analyze the flow of Newtonian and non-Newtonian fluids in eccentric annuli with inner-pipe rotation. Simulation results for Newtonian fluid in eccentric annuli showed (Fig. 2) increased pressure gradients as the rotation speed increases. This phenomenon is attributed to the inertial effect that arises from the coupling of Navier–Stokes equations as the flow becomes three-dimensional. Corresponding results for power-law fluid (Fig. 3) clearly indicated the influences of both inertial effect and shear thinning. The authors found that, in a slightly eccentric annulus (Fig. 3a), shear thinning dominates the counteracting inertial effect, whereas in a highly eccentric annulus (Fig. 3b), inertial effect becomes predominate. In an annulus of intermediate eccentricity, shear thinning and inertial effect become comparable and the influence of rotational speed becomes minimal.

Mathematical Modelling of Helical Flows in Concentric Annuli

Couette-Poiseuille/Helical flow of non-Newtonian fluid in concentric annulus was theoretically studied by a number of investigators.[26-28] Coleman and Noll[26] presented an analytical solution for a generalized fluid in concentric annulus considering both inner and outer cylinder rotations. This solution is adopted for YPL fluid and summarized in the last report.[29] Following the analytical treatment presented by Coleman and Noll[26], Luo and Peden[30] developed an exact solution for laminar flow of power-law fluids in annulus with pipe rotation. A set of equations was presented to describe a relationship between relevant dimensionless groups. The effect of each of the dimensionless group on the apparent viscosity profile, angular and axial velocities was analyzed.

Wei[7] conducted experimental and theoretical study to determine the effect of pipe rotation on friction pressure loss in concentric and eccentric annuli. The study followed a procedure similar to that of Luo and Peden[30] and presented numerical solutions for power-law fluid. Numerical results showed good agreement with the experimental measurements. All pressure loss measurements obtained from a concentric annulus with thick

muds indicated a reduction in pressure loss as the pipe rotation increased. However, for thin muds, the pipe rotation showed a positive effect on the pressure loss.

Stability Characteristics of Helical Flows

Helical flows between a rotating pipe and stationary outer cylinder often form translating or propagating spiral vortices. This is due to the centrifugal and shear instabilities that arise from the curved streamlines and the axial flow, respectively. Stability of a helical flow is characterized by the Taylor number and Reynolds number. The generalized Taylor number for annular flow of non-Newtonian fluids with a rotating inner pipe is given by[8]:

$$Ta = R_i (R_o - R_i)^3 \left(\frac{\rho \omega}{\mu_{app}} \right)^2 \quad \text{..... (1)}$$

The apparent viscosity, μ_{app}, in Equation (1) is estimated as:

$$\mu_{app} = \frac{\tau_y}{\dot{\gamma}_{\theta z}} + K \dot{\gamma}_{\theta z}^{m-1} \quad \text{.....} \quad (2)$$

where the combined average wall shear rate is given by:

$$\dot{\gamma}_{\theta z} = \sqrt{\dot{\gamma}_\theta^2 + \dot{\gamma}_z^2} \quad \text{.....} \quad (3)$$

where $\dot{\gamma}_z$ is the average axial wall shear rate, which is estimated according to the equivalent pipe model presented in previous report.[31] The average tangential wall shear rate, $\dot{\gamma}_\theta$, can be roughly estimated as:

$$\dot{\gamma}_\theta \approx \frac{\omega D_i}{D_o - D_i} \quad \text{.....} \quad (4)$$

The relevant Reynolds number to estimate the flow regime in eccentric annuli can be expressed as:

$$\mathrm{Re} = \frac{8 \rho U^2}{\bar{\tau}_w} \quad \text{.....} \quad (5)$$

The average wall shear stress, $\bar{\tau}_w$, can be obtained from the constitutive equation using the average axial wall shear rate.

Experimental Investigation

Test Setup

As previously reported, a vertical test section, which is fully transparent have been installed on the dynamic testing facility (DTF) to investigate the flow behavior of YPL fluids in annular flows with pipe rotation. The experimental setup for pipe rotation test and the associated instrumentation are shown in Fig. 4. The overall length of the test set section is approximately 10 ft [3 m]. The test section consists of a transparent outer cylinder (ID = 1½ inch / 38.1 mm) and interchangeable stainless steel pipe (OD = ½ inch / 12.7 mm, ¾ inch / 19 mm, and 1 inch / 25.4 mm). At the top and bottom, the inner pipe is supported by two sliding flanges to vary the eccentricity of the pipe. Three pressure taps (T1, T2 and T3) are located on the annular test section. The positions of the pressure tappings are shown in Fig. 4. Two differential pressure transducers ($\Delta P1=T1-T3$ and $\Delta P2=T2-T3$) are installed to measure the pressure gradient between the tappings. Water test were conducted before the pipe rotation experiments to verify the accuracy and reliability of the measurements. A detailed description of the test setup is available in the last report.[29]

Test Procedure

Experiments begin by filling the loop with warm water while the pump circulates the fluid at the lowest speed (146 rpm). When the loop is filled with water, the pump speed is increased to the maximum level to vent air pockets from the system. As the same time, air in the differential pressure transmitter lines is vented. The data acquisition system is turned on to monitor test parameters. Water is added or drained from the loop to provide the desired water level in the mixing tank. The fluid circulation through the pipe viscometer sections should be abandoned by opening the bypass valve (V3). Powder polymer and small quantity of glitter glue (i.e. decorative glue with small pieces of light-reflecting particles) are added gently, while water in the tank is being agitated and slowly circulated through the loop. The glitter glue particles help to identify the flow pattern. After sufficient time of mixing, the bypass valve will be closed. The test fluid flows though the horizontal sections; and then enters into the vertical test section at the bottom, flows upward, and leaves at the top, while the variable speed motor rotates the inner pipe at the desired speed. The pressure losses across the test sections, static pressure, temperature, and flow rate are continuously monitored and recorded by the data acquisition system. Rheologies of the fluids are determined using the horizontal test sections (pipe viscometers) and a rotational viscometer. Rotational speed of the inner pipe is measured using an optical tachometer, which is installed at the bottom of the test section.

During the test, the pressure losses are measured at different pipe rotation speeds while keeping other test parameters such as temperature and flow rate constant. Each rotational speed is maintained until steady state flow conditions were established.

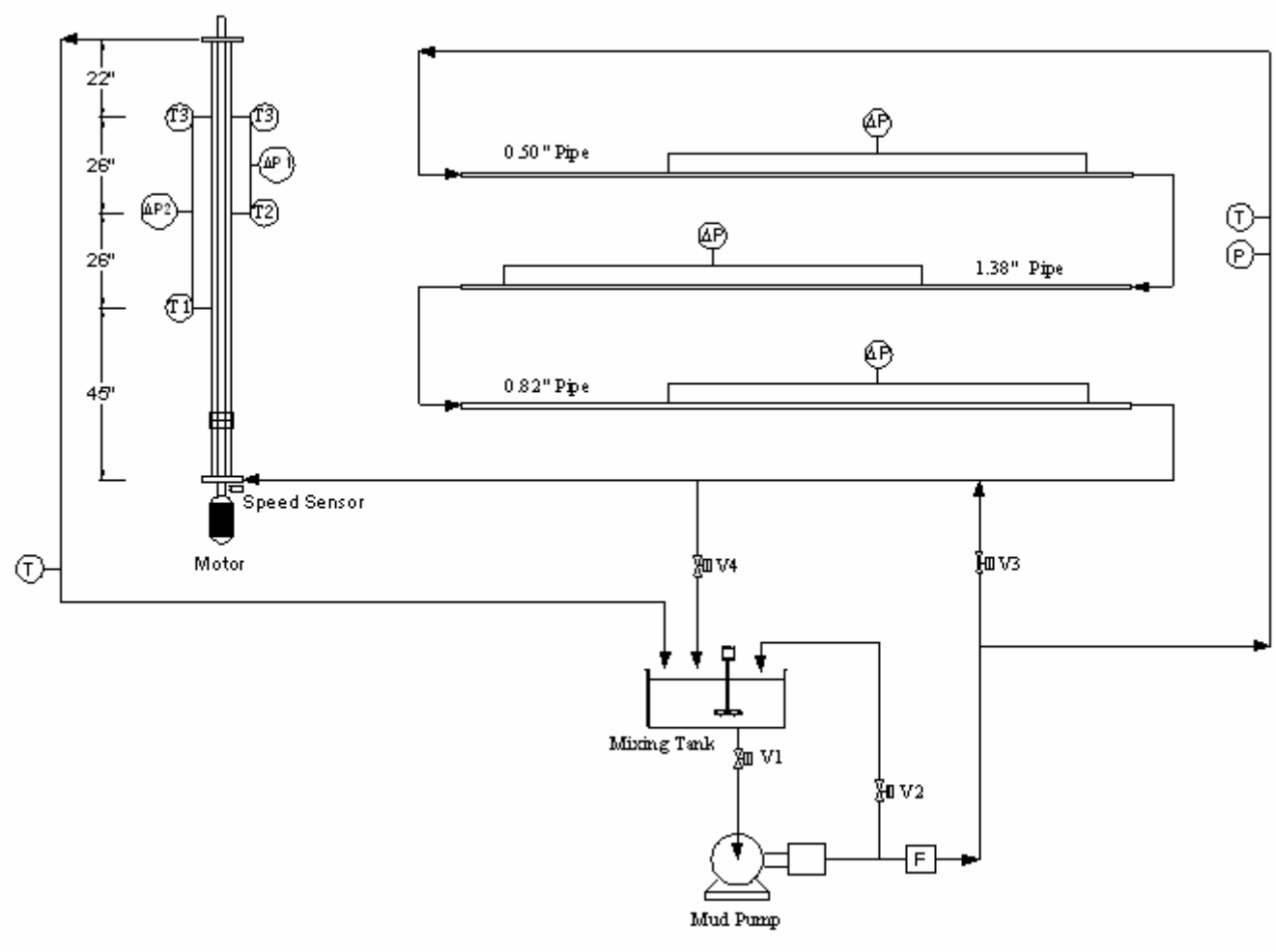

Fig. 4 Schematic of the Flow Loop for Pipe Rotation Tests

Experimental Results

For this investigation, polymeric fluids that were used in previous investigation[31] of pipe rotation are reconsidered. Five different formulations (Table 1) of test fluids were prepared by varying concentrations of Xanthan Gum (XCD) and Polyanionic Cellulose (PAC) in the system. Rheologies of test fluids that are presented in Table 2 and Table 3 were measured using pipe and rotational (Chan 35) viscometers, respectively. The densities of test fluids were approximately 8.33 ppg [1000 Kg/m^3].

The annular pressure gradient is measured using two differential pressure transducers (ΔP1 and ΔP2). For all the experiments, the measurements were approximately the same, which indicate the establishment of steady state flow condition.

Figure 5a through 5e show dimensionless annular frictional pressure loss measured in fully eccentric annulus (Annulus #1) as a function rotational speed for different mean flow velocities (flow rates) with different test fluids (i.e. A1, B1, C1, D1 and E1). The dimensionless annular frictional pressure loss is defined as:

$$\Delta p^{+} = \frac{g_c dP / dL}{g \cdot \rho_{H_2O}} \quad \text{.....} \quad (6)$$

where g_c, g and ρ_{H_2O} are the dimensional constant, gravitational acceleration and density of water, respectively. For the lowest flow velocity (0.15 m/s / 0.48 ft/s), the pressure gradients remains approximately constant as the rotation speed increases for the power-law fluids, A1 and B1. However, at higher flow rates, the pressure gradient slightly increased for these fluids.

In the case of the yield power-law fluids (C1, D1 and E1), the pressure gradient is decreased at low flow rates and increased at high flow rates. The effect of pipe rotation is minimal for the intermediate flow rates.

Previous measurements[31] in concentric annulus with the same annular geometry and similar fluids indicated that the pressure gradient predominantly decreases with the increase in the rotational speed. This could be due the shear thinning effect, which normally dominants in concentric and slightly eccentric annuli. However, in highly eccentric annuli, the shear thinning is counteracted by the inertial effect. Especially at high flow rate, the inertial effects due eccentric and annular irregularities overcome the shear thinning, resulting in an increase in the pressure gradient.

After completing the first set of experiments in Annulus #1, the ¾-inch pipe was replaced with a 1-inch pipe to investigate the influence of diameter ratio on the relationship between pipe rotation and the pressure loss. Both “concentric” and “fully eccentric” annular geometries were investigated. Table 4 compares the measured and predicted pressure losses in Annulus #2 with test Fluid A2 without pipe rotation. The predicted values are obtained using previously developed numerical procedure[31] for concentric annulus. Measured pressure losses are approximately 30% less than the predicted ones. The reduction in pressure loss is due to the pipe eccentricity. Small curvature of the inner or the outer pipe significantly affects the eccentricity of the annulus when the diameter ratio becomes high. As a result, it was not possible to place the inner pipe in perfectly concentric configuration.

Figures 6a through 6e present the pressure gradient measured in Annulus #2 with different test fluids (i.e. A2, B2, C2, D2 and E2). The results for the power-law fluids (A2 and B2) indicate that the effect of pipe

rotation on the pressure loss is positive at low speeds (0 to 200 rpm). This is mainly due to the inertial effect, which is generated due to small eccentricity of the inner pipe and geometric irregularities of the annulus. However, at higher speeds, the shear-thinning phenomenon counteracts the inertial effect. The combined effect of these two phenomena results in reduction of pressure loss at higher rotational speeds (200 rpm to 400 rpm) as the speed increases.

For fluids with high yield stress (Fluid C2 and D2), at low flow rates, the pressure gradient decreases because of the shear thinning. Nonetheless, at high flow rates, the inertial effects overcome the influence of shear thinning; as a result, the pressure gradient increases as the rotation speed increases. For intermediate flow rates, the patterns of the pressure gradient curves are similar to that of the power-law fluid (Fluid A2). Results of Fluid E2 (Fig. 6e) show that the pressure gradients for high flow rates (6.77 ft/s and 5.88 ft/s) decrease as the rotational speeds increases from 0 to 100 rpm, then it decreases as the rotation speed increases. It is important to note that the Reynolds numbers (Table 6) for these flow rates are close to 2100. For intermediate flow rates, the patterns of pressure gradient curves are not same as that of high flow rates and the pressure gradient steadily increases (maximum 21%) as pipe rotation increases.

After conducting sufficient tests in Annuls #2, the eccentricity of the inner pipe was increased to obtain a fully eccentric configuration (i.e Annuls #3). Figures 7a through 7e present the pressure gradient measured in Annulus #3 with five different test fluids. At the lowest flow rate, slight decrease in pressure loss is observed as the rotation increases. For other flow rates, the annular pressure loss predominantly increases with the increase in pipe rotation. At the highest flow rates, measurements with fluids B3 and E3 indicate significant reduction (approximately 15%) in pressure loss when the pipe begins to rotate at 50 rpm. This reduction in pressure loss could be due to the effect of geometric irregularities of the annulus, which has the influence on the pressure loss depending on the angular position of the inner pipe. In order to investigate the variation of pressure loss with the angular position of the inner pipe, pressure loss measurements were performed at different angular positions keeping the flow rate constant (Fig. 8). The results obtained at different flow rates (6 gpm and 14 gpm) suggested that the pressure loss measurements without pipe rotation have significant discrepancy, which can be as high as 35 percent. Even though these discrepancies are minimized taking average values of measurements obtained at two randomly selected positions of the inner pipe, in some cases high discrepancies may be observed. The influence of angular position on the pressure loss is dependent on the geometry irregularity of the annulus and diameter ratio. The measurement discrepancies in Annuls #1 that has diameter ratio of 50% were 10% maximum.

Figures 9, 10 and 11 show pressure loss ratio (i.e. $R = \Delta p_{\omega}/\Delta p_{\omega=0}$) as a function of Taylor number in Annulus #1, #2 and #3, respectively. Measurements in fully eccentric annuli (Figs. 9 and 11) show significant

increase (up to 50%) in pressure loss due to pipe rotation. However, in few cases, slight reductions in pressure losses have been observed. In Annulus #2, the pressure loss ratio ranges from 0.6 to 1.17 (Fig. 10).

Conclusions

Laminar flow of Yield Power-Law fluid in eccentric annulus with pipe rotation was investigated experimentally. Annular pressure losses were predominately measured under laminar flow conditions. From the results of this investigation, the following conclusion can be drawn.

- Results indicate the presence of shear thinning and inertial effects when inner pipe rotates. In highly eccentric annuli, inertial effects largely dominate the phenomena of shear thinning and results in increased pressure loss as the pipe rotates.
- Inertial effects can be generated due eccentricity and/or geometric irregularities of the annulus that substantially affects the velocity field as the pipe rotates.
- It is important to note that flow measurements under relatively controlled experimental setup still show the presence of geometric irregularities, which can generate significant increase in pressure loss as the pipe rotates. In the field, this phenomenon may considerably affect the annular pressure loss when the drill pipe rotates.

Future work

i) Our next plan is investigation of the effects of pipe rotation and temperature on the friction pressure loss.
ii) Experimental investigation of the rheology and hydraulics of YPL (synthetic/polymeric/bentonite) fluids under different temperature conditions;
iii) Study the effect of pressure on rheology and hydraulics of YPL (synthetic/polymeric) fluids under laminar flow conditions;
iv) Investigation on turbulent flow of YPL fluids in pipes and annuli;
v) Study the effects wall roughness on frictional pressure losses under turbulent flow conditions;
vi) Investigation on the effects of pipe rotation and eccentricity under turbulent flow conditions;
vii) CFD simulations;
viii) Development of guidelines and a hydraulic simulator for ECD management and hydraulics optimization.

Nomenclature

D = pipe diameter

f = friction factor

K = Fluid's Consistency Index

L = Pipe Length

m = Fluid Behavior Index

N = Generalized Fluid's Behavior Index

Q = Volumetric Flow Rate

R = Diameter Ratio

Re = Reynolds number

Ta = Taylor number

U = axial mean flow velocity

Greek Letters

Δ = difference

$\dot{\gamma}$ = Shear Rate

ω = angular speed

τ = Shear Stress

Subscripts

eff = effective

i = inside

o = outside

y = yield

w = wall

References

[1] Davison, J. M., Clary, S., Saasen, A., Allouche, M., Bodin, D. and Nguyen, V-A. "Rheology of Various Drilling Fluid Systems under Deepwater Drilling Conditions and the Importance of Accurate Predictions of Downhole Fluid Hydraulics" SPE paper 56632, presented at SPE Annual Technical Conference and Exhibition, 3-6 October, Houston.

[2] Friedheim, J.E. and Conn, H.L. 1996, "Second Generation Synthetic Fluids in the North Sea: Are They Better?", SPE paper 35061, Presented at IADC/SPE Drilling Conference held in New Orleans, Louisiana, 12-15 March.

[3] Yamada, Y. "Resistance of a flow through an annulus with an inner rotating cylinder," Bull. JSME, 5, No. 18, 1962, pp. 302–310.

[4] Walker, R.E. and AI-Rawi, R. "Helical Flow of Bentonite Slurries", SPE 3108, presented at the 45th Ann. Fall Meeting of the SPE of AIME in Houston, October 4-7, 1970.

[5] Nouri, J. M., and Whitelaw, J. H. "Flow of Newtonian and Non-Newtonian Fluids in a Concentric Annulus with Rotation of the Inner Cylinder," ASME J. Fluids Eng., 1994, 116, pp. 821–827.

[6] Hansen, S. A., Sterri, N. "Drill Pipe Rotation Effects on Frictional Pressure Losses in Slim Annuli," SPE paper 30488, presented at the SPE Annual Technical Conference and Exhibition, 22-25 October, 1995, Dallas, Texas.

[7] Wei, X. “Effects of Drillpipe Rotation on Annular Frictional Pressure Loss in Laminar, Helical Flow of Power-Law Fluids in Concentric and Eccentric Annuli,” MSc. Thesis, the University of Tulsa, 1997.

[8] Hansen, S. A., Rommetveit, R., Sterri, N., Aas, B. and Merlo, A. “A New Hydraulics Model for Slim Hole Drilling Applications,” SPE paper 57579, presented at the SPE/IADC Middle East Drilling Technology Conference, 8-10 November, 1999, Abu Dhabi, United Arab Emirates.

[9] Woo, N. Seo, B.and Hwang, Y. “Flow of Newtonian and Non-Newtonian Fluids in Annuli with Rotating Inner Cylinder,” 6th World Conference on Experimental Heat Transfer, Fluid Mechanics, and Thermodynamics, April 17-21, 2005, Matsushima, Miyagi, Japan.

[10] Bode, D.J., Noffke, R.B., Nickens, H.V., “Well-Control Methods and Practices in Small-Diameter Wellbores,” SPE 19526, JPT, Nov. 1991, 1380-1386.

[11] Delwiche, R.A., Stratabit. DB, Lejeune, M.W.D., Mawet, P.F.B.N., Vighetto, R. “Slimhole Drilling Hydraulics,” SPE Paper 24596, presented at the SPE Annual Technical Conference and Exhibition, 4-7 October, 1992, Washington, D.C.

[12] Marken, C.D., He, X., Saasen, A. “The Influence of Drilling Conditions on Annular Pressure Losses,” SPE paper 24598, SPE Annual Technical Conference and Exhibition, 4-7 October, Washington, D.C. 1992.

[13] McCann, R.C., Quigley, M.S., Zamora, M. and Slater, K. ”Effects of High-Speed Pipe Rotation on Pressures in Narrow Annuli," SPE 26343, presented at the 1993 SPE ACTE in Houston, October 3-6.

[14] Wang, H., Su, Y., Bai,Y., Gao, Z. and Zhang, F. “Experimental Study of Slimhole Annular Pressure Loss and Its Field Applications,” SPE paper 59265, presented at the IADC/SPE Drilling Conference, 23-25 February, 2000, New Orleans, Louisiana.

[15] Diaz, H., Miska, S., Takach, N. and Yu, M. “Modeling of ECD in Casing Drilling Operations and Comparison with Experimental and Field Data,” SPE 87149, presented at the IADC/SPE Drilling Conf. Dallas, 2–4 March 2004.

[16] Diaz, H.J. “Field Experimental Study and Modeling of ECD in Casing Drilling Operations,” MSc. Thesis, the University of Tulsa, 2002.

[17] Ward, C. and Adreassen, E. “Pressure While Drilling Data Improve Reservoir Drilling Performance," SPE Drilling and Completion, 13:1, 19-24 March, 1998.

[18] Isambourg, P., Bertin, D. and Branghetto, M. “Field Hydraulic Tests Improve HPHT Drilling Safety and Performance,” SPE Drilling and Completion, 14:4, 219-227, December 1999.

[19] Luo, Y. and Peden, J.M. “Flow of Drilling Fluids through Eccentric Annuli,” paper SPE 16692, presented at the 62nd SPE ACTE in Dallas, September 27-30, 1987.

[20] Hemphill, T. and Ravi, K. "Calculation of Drillpipe Rotation Effects on Axial Flow: An Engineering Approach," SPE 97158, presented at the 2005 SPE Ann. Tech. Conf., 9-12 October, Dallas.

[21] Wan, S., Morrison, D. and Bryden, I.G. "The Flow of Newtonian and Inelastic Non-Newtonian Fluids in Eccentric Annuli with Inner-Cylinder Rotation," Theoret. Comput. Fluid Dynamics (2000) 13: 349–359.

[22] Fang, P. and Manglik, R. M. "The Influence of Inner Cylinder Rotation on Laminar Axial Flows in Eccentric Annuli of Drilling Bore Wells," Int. J. of Tran. Phenomena, Vol. 4, No. 4, 2002, 257-274.

[23] Escudier, M.P. Oliveira, P.J. Pinho, F.T. "Fully developed laminar flow of purely viscous non-Newtonian liquids through annuli including the effects of eccentricity and inner-cylinder rotation," Int. J. Heat and Fluid Flow. Vol. 23, 2002, 52-73.

[24] Meuric, O.F.J. , Wakeman, R.J., Chiu, T.W. and Fisher, K.A. "Numerical Flow Simulation of Viscoplastic Fluids in Annuli," The Canadian Journal of Chem. Engineering, Vol. 76, Feb., 1998.

[25] Andres S.A. and Szeri, A.Z. "Flow between eccentric rotating cylinders," Journal of applied mechanics, vol. 51, no 4, pp. 869-878, 1984.

[26] Coleman, B.D. and Noll, W. "Helical Flow of General Fluids," J. of App. Phy., Oct. 1959, Vol. 30, Issue 10, pp. 1508-1512.

[27] Fredrickson, A.G. and Bird, R.B., 1958, "Non-Newtonian Flow in Annuli", Ind. Eng. Chem., 50, 347-383.

[28] Savins, J. G. and Wallick,G. C. "Viscosity profiles, discharge rates, pressures, and torques for a rheologically complex fluid in a helical flow," AIChE Journal, Vol. 12, Issue 2 , Pages 357 – 363.

[29] Ahmed, R. "Experimental Study and Modeling of Yield Power-Law Fluid Flow in Pipes and Annuli," TUDRP ABM report, May 2006.

[30] Luo, Y. and Peden, J.M. "Reduction of the Annular Friction Pressure Drop Caused by Drillpipe Rotation," SPE 20305, Society of Petroleum Engineers, 1990.

[31] Ahmed, R. "Experimental Study and Modeling of Yield Power-Law Fluid Flow in Pipes and Annuli," TUDRP ABM report, Nov 2005.

Table 1 Annular Geometries and Test Fluid Compositions

Fluid Rheology	Annular Geometry			Nominal Concentration by Weight	
	1½" × ¾" Fully Eccentric (Annulus #1)	1½" × 1" Concentric (Annulus #2)	1½" × 1" Fully Eccentric (Annulus #3)	XCD	PAC
Power-Law (PL)	Fluid A1	Fluid A2	Fluid A3	0.50%	0.90%
	Fluid B1	Fluid B2	Fluid B3	0.25%	0.45%
Yield Power Law (YPL)	Fluid C1	Fluid C2	Fluid C3	1.50%	0.00%
	Fluid D1	Fluid D2	Fluid D3	0.70%	0.00%
	Fluid E1	Fluid E2	Fluid E3	0.30%	0.00%

Table 2 Rheological Properties of Test Fluids Measured Using Pipe Viscometer

Test Fluid	τ_y		K		m	Temp.
	[lbf/100ft^2]	[Pa]	[lbf/100ft^{2}s^m]	[Pas^m]		[°F]
A1	0.00	0.00	1.74	0.84	0.53	78-87
B1	0.00	0.00	0.52	0.25	0.61	98-101
C1	21.93	10.50	2.03	0.97	0.53	77-84
D1	10.44	5.00	0.71	0.34	0.58	96-99
E1	4.18	2.00	1.16	0.56	0.42	104-113
A2	0.00	0.00	1.74	0.83	0.56	75-85
B2	0.00	0.00	0.73	0.35	0.59	72-81
C2	22.97	11.00	2.18	1.05	0.52	80-88
D2	10.44	5.00	0.82	0.39	0.52	89-90
E2	1.04	0.50	0.56	0.27	0.47	82-84
A3	0.00	0.00	1.93	0.93	0.52	90-93
B3	0.00	0.00	0.78	0.37	0.59	81-86
C3	14.62	7.00	3.56	1.71	0.44	78-83
D3	6.47	3.10	1.54	0.74	0.48	90-94
E3	3.13	1.50	0.62	0.30	0.52	94-99

Table 3 Dial Readings from Rotational Viscometer (Chan 35) in lbf/100ft^2

Test Fluid	Temp.	Speed [rpm]											
	[°F]	1	2	3	6	10	20	30	60	100	200	300	600
A1	77	1.0	2.0	3.0	5.0	6.0	10.0	13.0	21.0	28.0	41.0	51.0	71.0
B1	98	1.0	1.5	2.0	2.5	3.0	5.0	6.0	9.0	12.0	19.0	24.0	36.0
C1	76	23.0	26.0	27.0	31.0	34.0	39.0	42.0	50.0	57.0	70.0	79.0	99.0
D1	93	8.5	10.0	11.0	13.0	14.5	17.0	19.0	23.0	27.0	33.0	38.0	51.0
E1	100	3.0	3.5	4.0	4.5	5.5	6.5	7.5	9.5	11.0	14.0	16.0	21.0
A2	85	2.5	4.0	5.0	9.0	10.0	14.0	17.5	25.0	33.0	46.0	56.0	76.0
B2	80	1.0	1.5	2.0	3.0	4.0	6.0	8.0	11.0	15.0	22.0	27.0	40.0
C2	87	22.0	25.0	26.0	29.0	31.0	35.0	38.0	43.0	48.0	57.0	63.0	79.0
D2	88	7.0	8.5	10.0	11.5	13.0	16.0	18.0	21.0	24.0	30.0	35.0	44.0
E2	81	1.0	2.0	2.0	3.0	3.0	4.0	5.0	6.0	8.0	10.0	11.0	16.0
A3	89	4.5	5.0	6.0	8.0	10.0	14.0	16.0	25.0	32.0	43.0	51.0	70.0
B3	80	1.0	1.5	2.0	3.0	4.0	6.0	8.0	11.0	15.0	23.0	29.0	41.0
C3	80	20.0	23.0	25.0	28.0	31.0	35.0	38.0	45.0	51.0	63.0	72.0	93.0
D3	90	8.5	10.0	11.0	13.0	14.0	16.0	18.0	22.0	26.0	33.0	38.0	50.0
E3	93	3.5	4.0	4.5	5.5	6.5	8.0	9.0	11.0	13.0	17.0	20.0	28.0

Table 4 Measured and Predicted Pressure Gradient in Annulus #2 with Fluid A2 without Pipe Rotation

Q [GPM]	Measured [Dimensionless]	Predicted [Dimensionless]	Difference
0.55	0.18	0.27	35%
1.99	0.41	0.56	27%
6.01	0.78	1.04	24%
9.97	1.01	1.37	27%
14.02	1.15	1.66	31%
18.01	1.39	1.91	27%
20.34	1.43	2.04	30%

Table 5 Reynolds Numbers at Different Flow Rates in Annulus #1

Q [GPM]	U [m/s]	U [ft/s]	Fluid A1	Fluid B1	Fluid C1	Fluid D1	Fluid E1
2	0.15	0.48	30.90	76.96	10.34	23.76	37.98
6	0.44	1.45	155.75	359.86	70.55	155.10	641.39
10	0.74	2.42	324.12	734.72	172.00	365.43	1136.32
14	1.03	3.39	524.93	1153.34	301.10	636.97	1726.17
18	1.33	4.36	754.67	1613.51	456.60	958.41	2262.32
Max	Max	Max	942.47	-	456.60	-	-

Table 6 Reynolds Numbers at Different Flow Rates in Annulus #2

Q [GPM]	U [m/s]	U [ft/s]	Fluid A2	Fluid B2	Fluid C2	Fluid D2	Fluid E2
2	0.20	0.65	2.86	7.08	0.70	2.01	6.30
6	0.60	1.96	18.13	38.33	9.77	24.89	76.88
10	1.00	3.27	89.49	174.07	60.83	155.22	432.05
14	1.39	4.58	186.07	359.94	139.27	357.93	962.20
18	1.79	5.88	304.50	579.93	241.81	618.24	1608.26
Max	Max	Max	436.90	828.31	359.26	926.39	2375.62

Table 7 Reynolds Numbers at Different Flow Rates in Annulus #3

Q [GPM]	U [m/s]	U [ft/s]	Fluid A3	Fluid B3	Fluid C3	Fluid D3	Fluid E3
2	0.20	0.65	4.42	11.73	2.06	1.28	10.39
6	0.60	1.96	38.83	71.36	19.35	38.77	80.03
10	1.00	3.27	195.84	331.12	122.64	239.25	474.88
14	1.39	4.58	418.26	684.82	289.34	544.03	1065.34
18	1.79	5.88	684.08	1101.43	504.77	940.95	1803.59
Max	Max	Max	994.33	1558.39	756.20	1395.43	2665.53

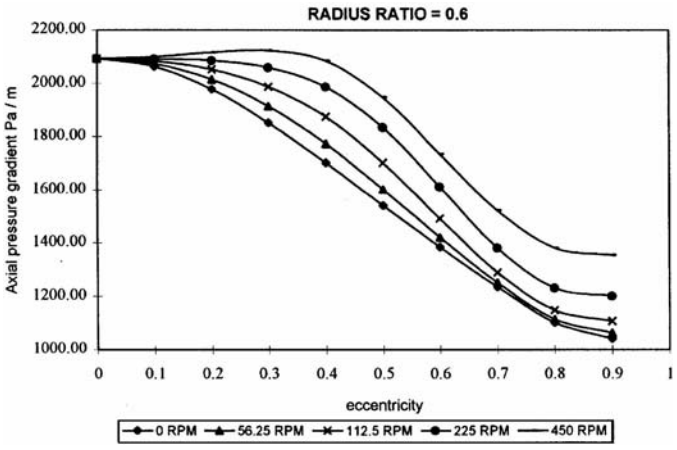

Fig. 2 Predicted Pressure Gradient vs. Eccentricity for Various Inner-cylinder Rotation Speeds for Newtonian fluid (after *Wan et al*.[21])

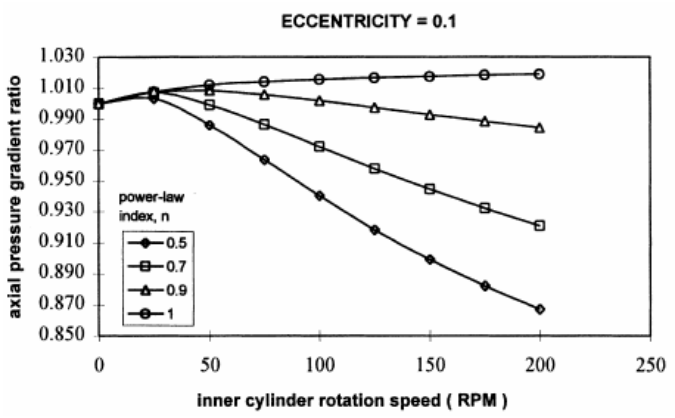

(a)

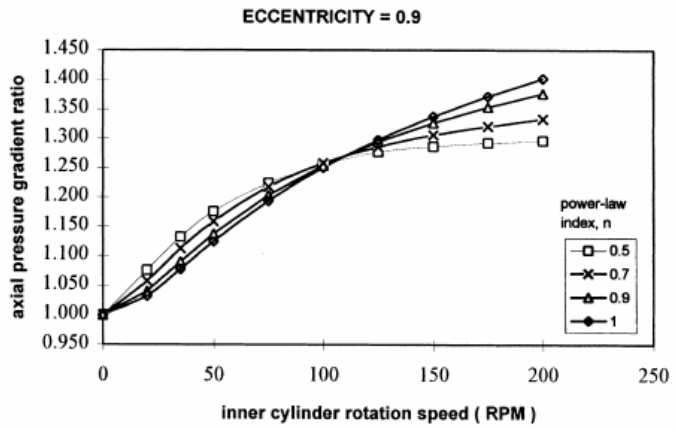

(b)

Fig. 3 Predicted Pressure Gradient vs. Eccentricity for Various Inner-cylinder Rotation Speeds for Power-law fluid (after Wan *et al*.[21])

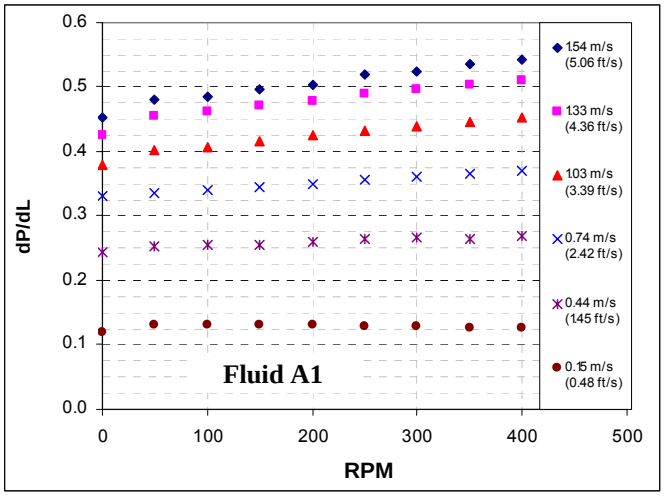

(a)

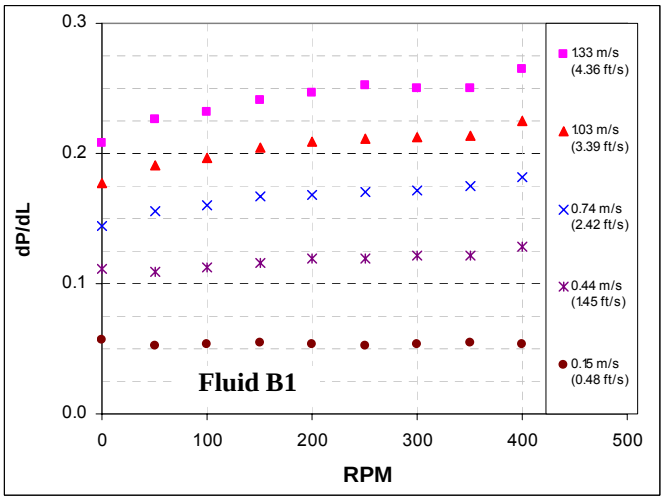

(b)

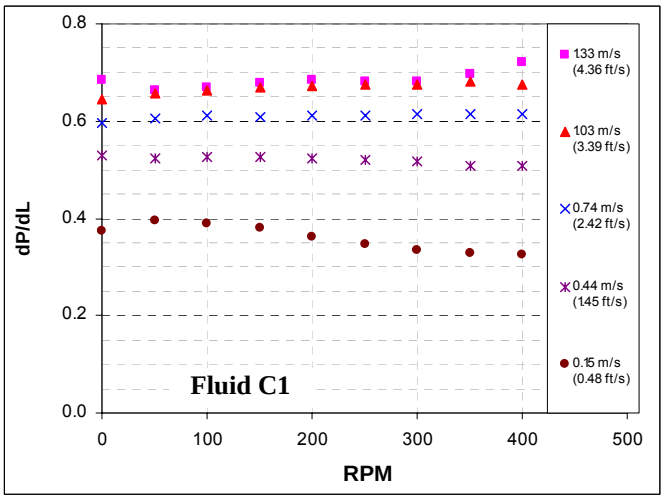

(c)

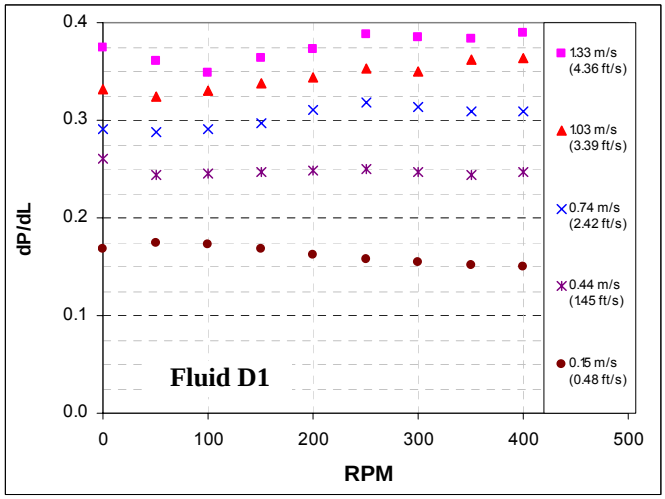

(d)

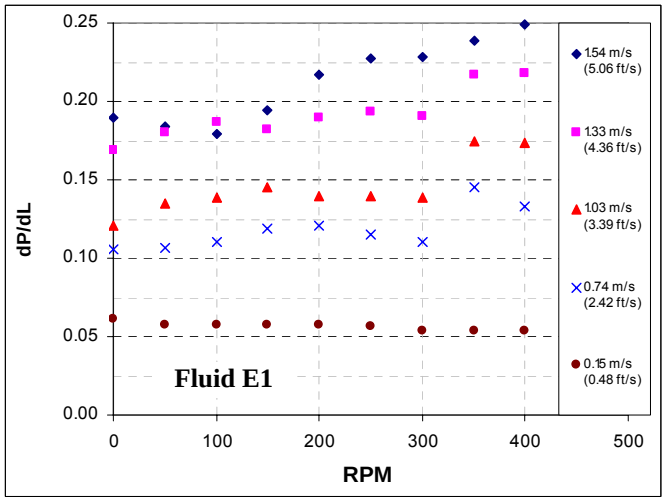

(e)

Fig. 5 Dimensionless Pressure Gradient vs. RPM for Different Flow Velocities in Fully Eccentric Annulus #1 with: a) Fluid A1; b) Fluid B1; c) Fluid C1; d) Fluid D1; and e) Fluid E1.

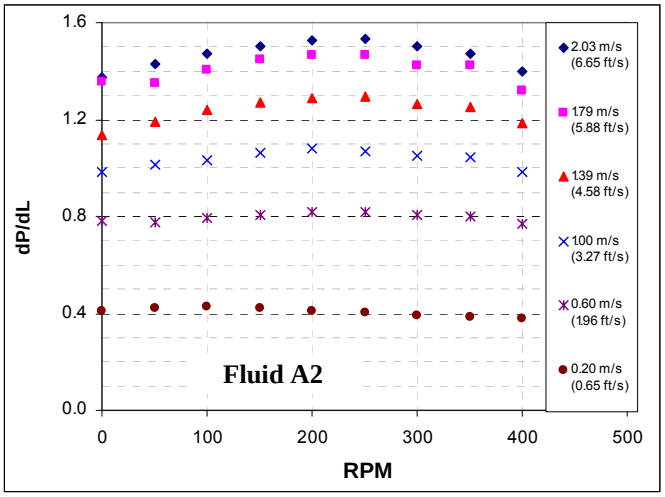

(a)

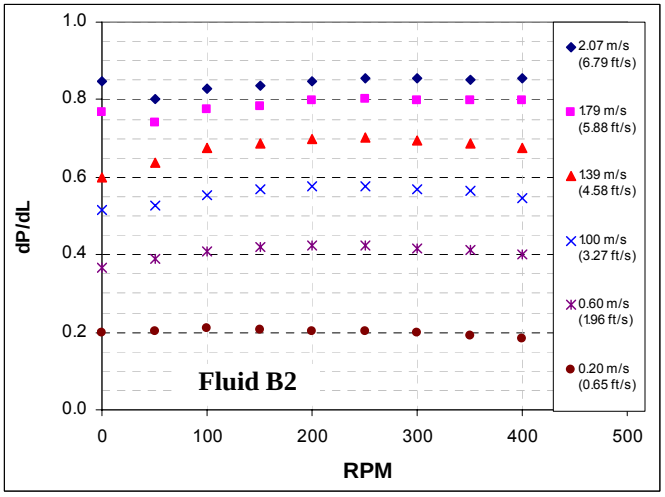

(b)

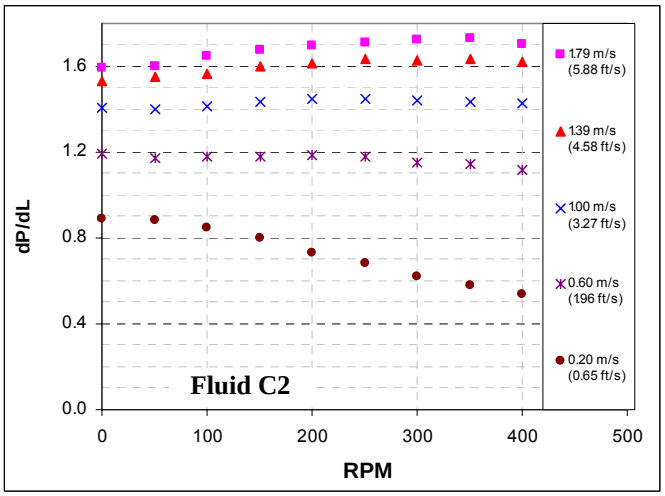

(c)

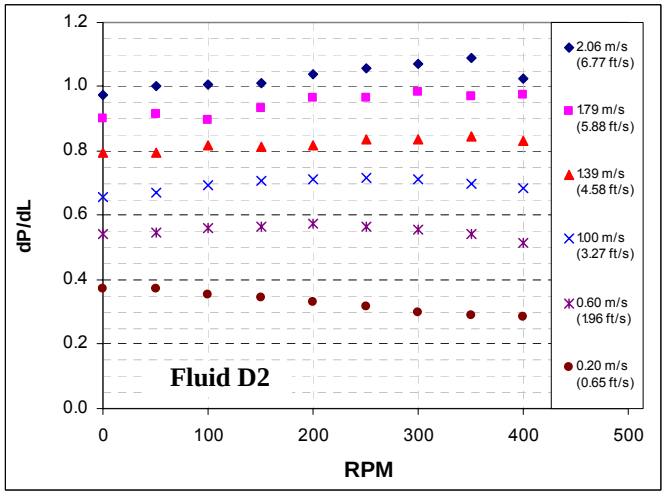

(d)

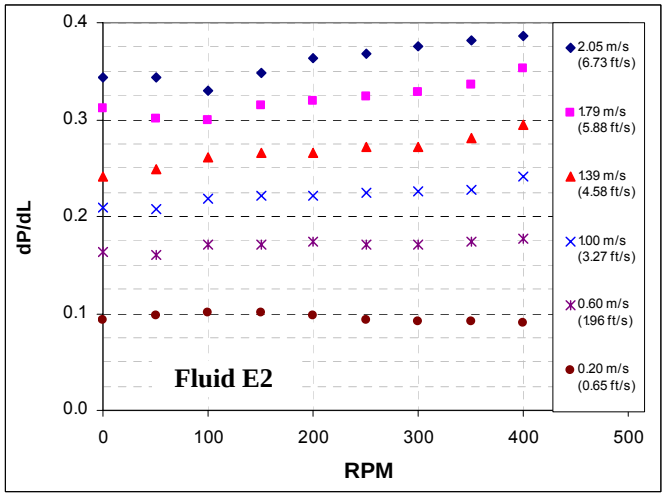

(e)

Fig. 6 Dimensionless Pressure Gradient vs. RPM for Different Flow Velocities in Annulus #2 with: a) Fluid A2; b) Fluid B2; c) Fluid C2; d) Fluid D2; and e) Fluid E2.

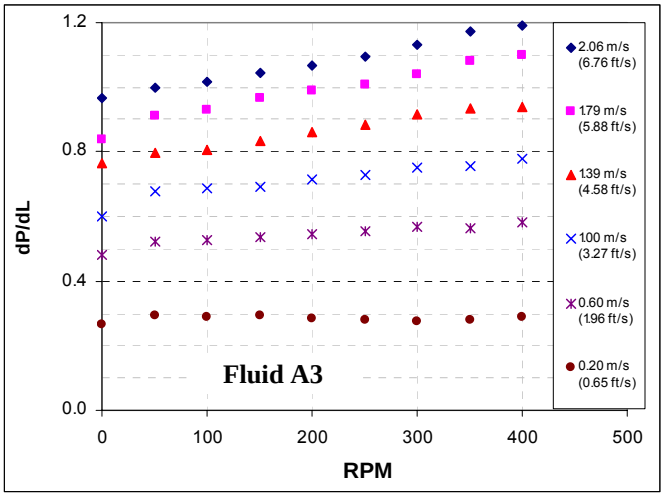

(a)

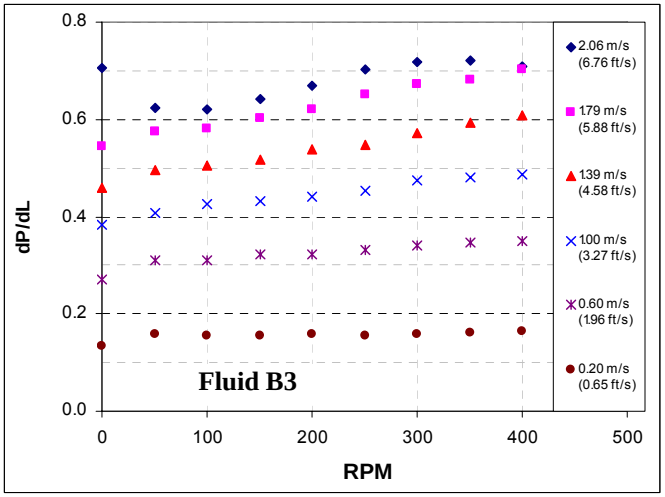

(b)

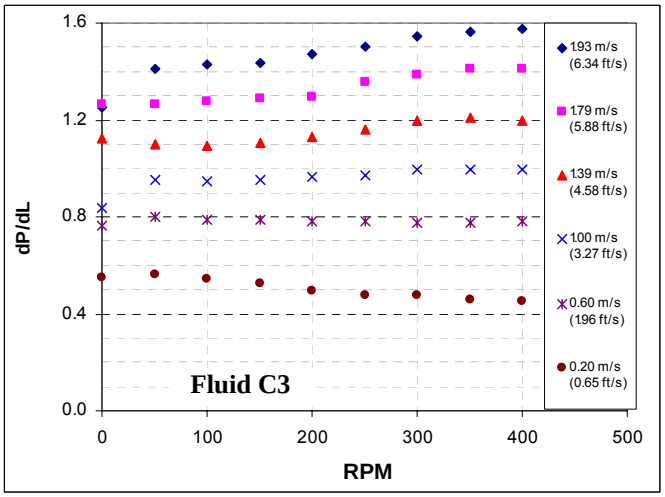

(c)

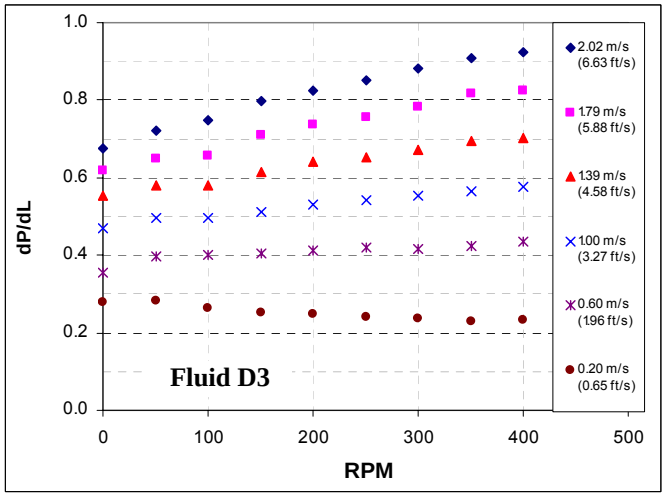

(d)

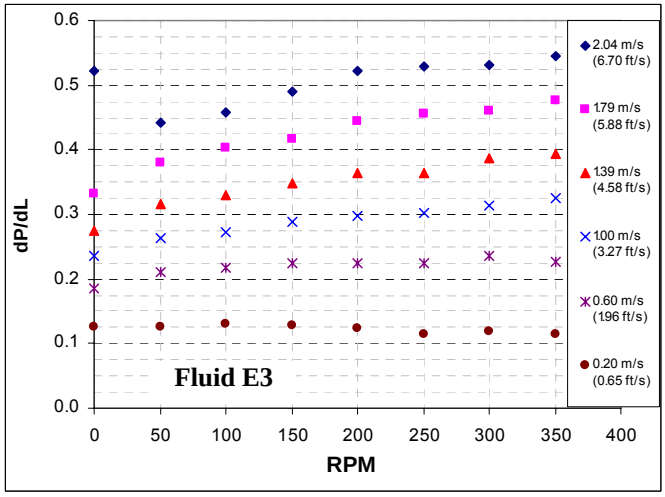

(e)

Fig. 7 Dimensionless Pressure Gradient vs. RPM for Different Flow Velocities in Fully Eccentric Annulus #3 with: a) Fluid A3; b) Fluid B3; c) Fluid C3; d) Fluid D3; and e) Fluid E3.

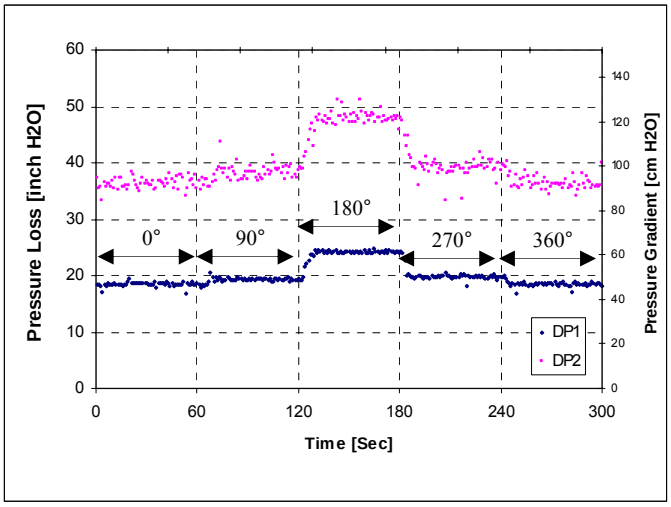

Fig. 8 Pressure Loss at Different Angular Positions for Fluid E3 at 6 GPM in Annulus #3

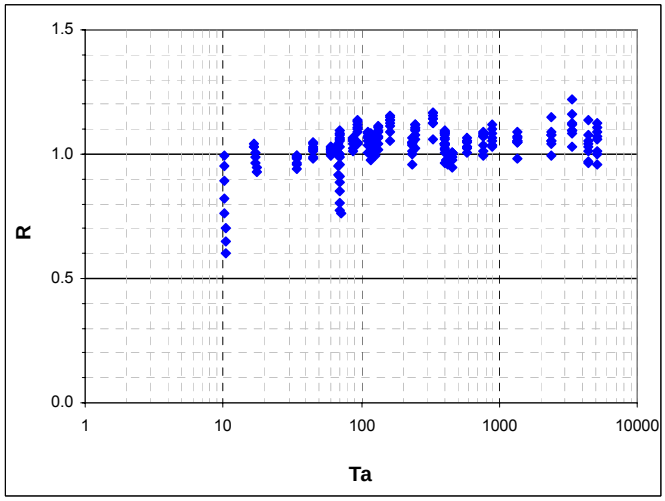

Fig. 10 Pressure Loss Ratio as a Function of Taylor Number in Annulus #2 with Fluid A2, B2, C2, D2 and E2

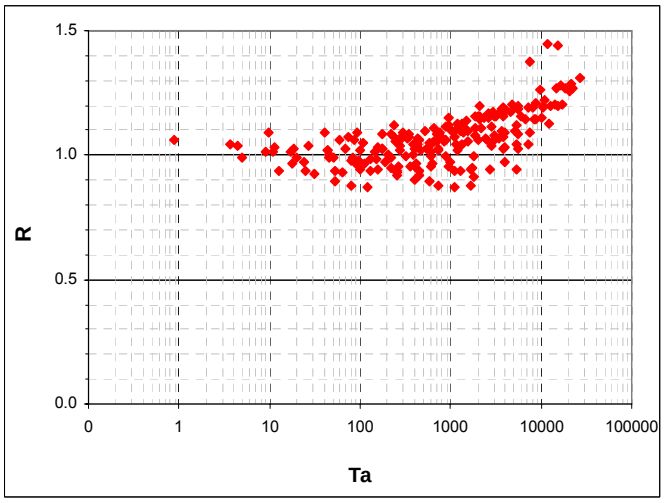

Fig. 9 Pressure Loss Ratio as a Function of Taylor Number in Annulus #1 with Fluid A1, B1, C1, D1 and E1

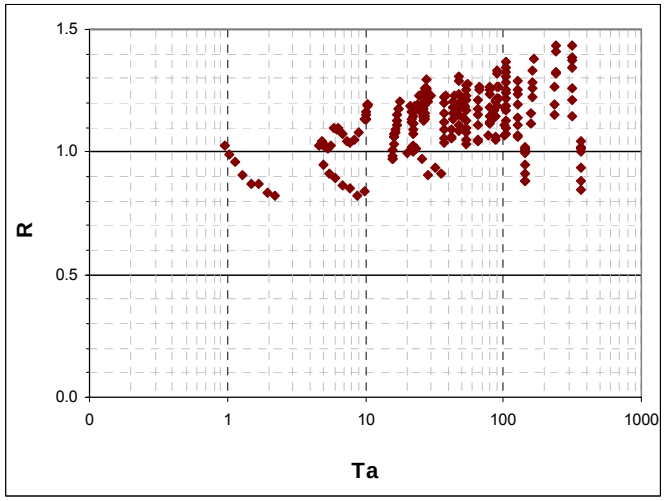

Fig. 11 Pressure Loss Ratio as a Function of Taylor Number in Annulus #3 with Fluid A3, B3, C3, D3 and E3